

Stress transfer and fault geometry's influence on the 2019 Ridgecrest Earthquake slip distribution

Jordan Cortez¹, Christodoulos Kyriakopoulos², Baoning Wu¹, David Oglesby¹, Roby Douilly¹, Kuntal Chaudhuri¹, Abhijit Ghosh¹

¹University of California, Riverside, ² University of Memphis



Abstract

Stress transfer from long-term loading as well as prior earthquakes can lead to seismic triggering and strongly affect subsequent rupture propagation and slip patterns in a fault system. A prime example of this effect is the 2019 Ridgecrest earthquake sequence, which consisted of multiple complex conjugate fault ruptures with delayed rupture triggering. On July 4th, 2019 an M6.4 earthquake produced left lateral surface ruptures as well as slip on a buried right-lateral conjugate fault. Approximately 30 hours later an M5.4 earthquake occurred ~10km northwest of the M6.4 hypocenter; then 6 hours later an M7.1 main shock occurred almost 2 km west of the M5.4 event. In this study, we utilize 3D finite element dynamic rupture models of the M6.4 and M7.1 events and compare models with different initial stress conditions to better understand how complex geometry and stress can influence rupture propagation, and hence overall slip patterns. These effects are extremely sensitive to the fault geometry, so our models are constrained by both observed surface ruptures and aftershock data. We model the M7.1 event using both constant traction initial stresses as well as the residual stress pattern transferred from the earlier M6.4 event. Our results suggest both homogenous and heterogenous initial stress models of the M7.1 main shock produce heterogenous slip for that event, but the latter model produces slip patterns that agree more with geodetic models. Both models illustrate the influence fault geometry has on rupture propagation, with varying slip patterns near bends and fault intersections. Overall, our study illustrates that slip on the fault is strongly affected by both the initial stress field and the details of fault geometry. Investigating the physical mechanisms associated with the seismic “domino effect” will improve our knowledge regarding fault interactions and help estimate their effects in potential future events.

Region of Interest

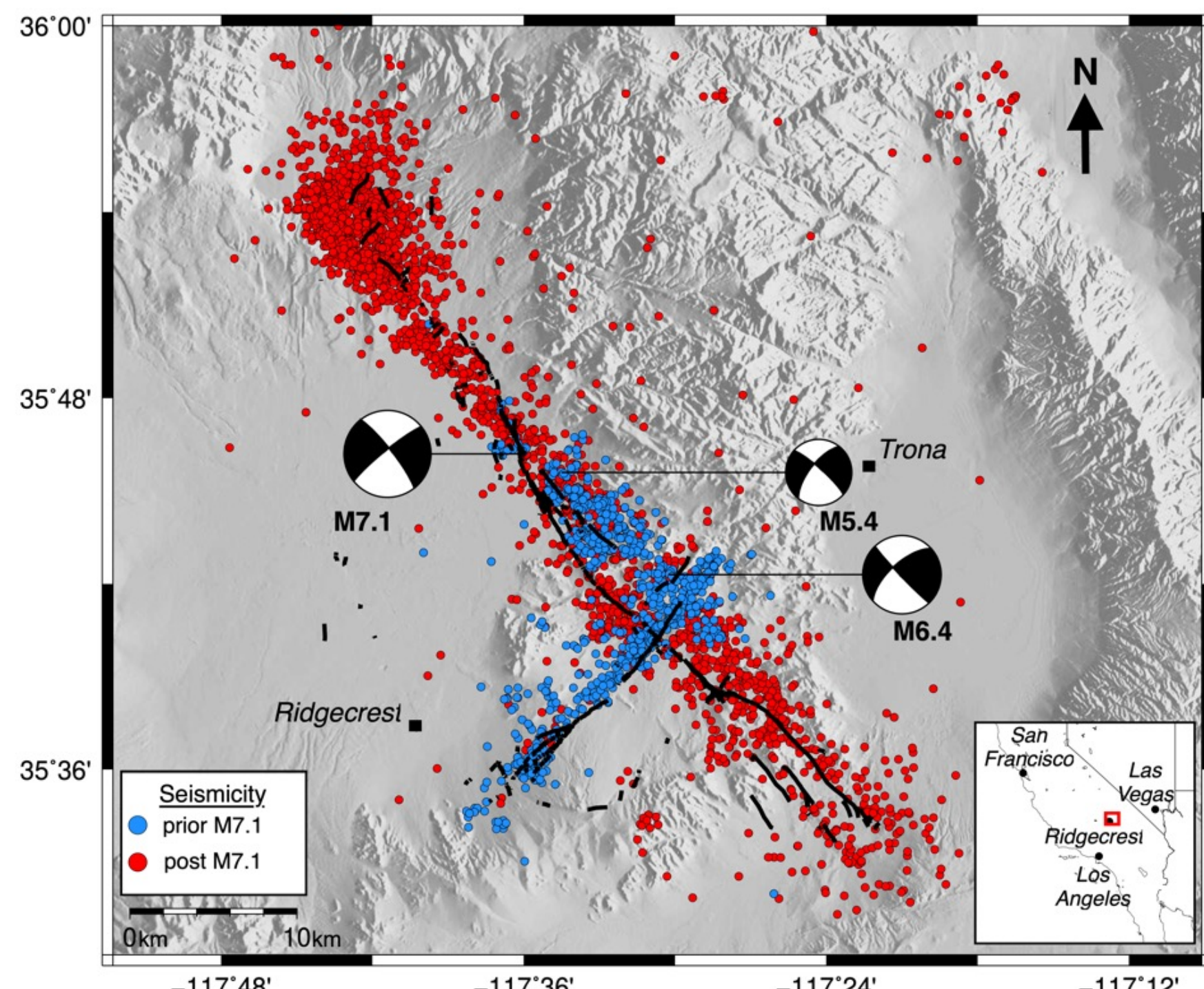


Fig. 1 Mapped surface rupture (black curves), main earthquakes displayed by Focal mechanisms, and aftershocks color-coded by timing with respect to the M7.1 event.

Methodology

Trelis

The fault system mesh in fig 3, consisting of 4 million hexahedral elements with sizes of 200m near the rupture area and 600 m in the outer region, was created using Trelis software.

FaultMod

We utilize the 3D dynamic finite element method FaultMod (Barrell 2009), which incorporates a slip weakening friction law, to model the M7.1 events. The constant traction models use the stress parameters in the table on the right. The heterogeneous models use the stress parameters as an envelope but are modified by the residual stress transferred from our model of the M6.4 event (Cortez et al., 2021).

Geodetic and Seismic Inversions: Slip distributions along M7.1 fault

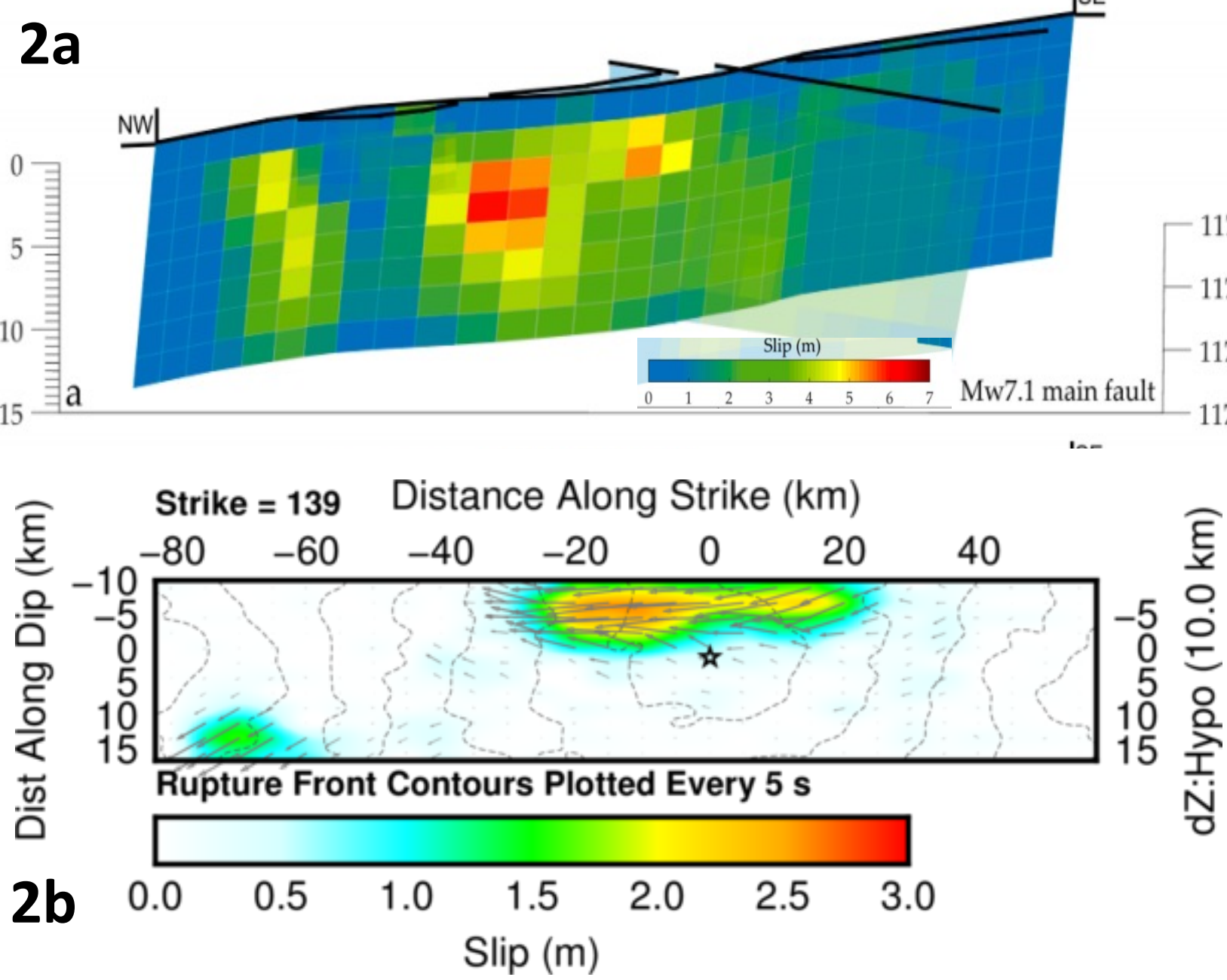


Fig 2a. Slip distributions for the M7.1 event using optical images and InSAR displacement constraints (Li et al., 2020). **Fig 2b** Seismic inversion of the M7.1 event using a finite fault inverse algorithm (Ji et al., 2002) and the USGS waveform database.

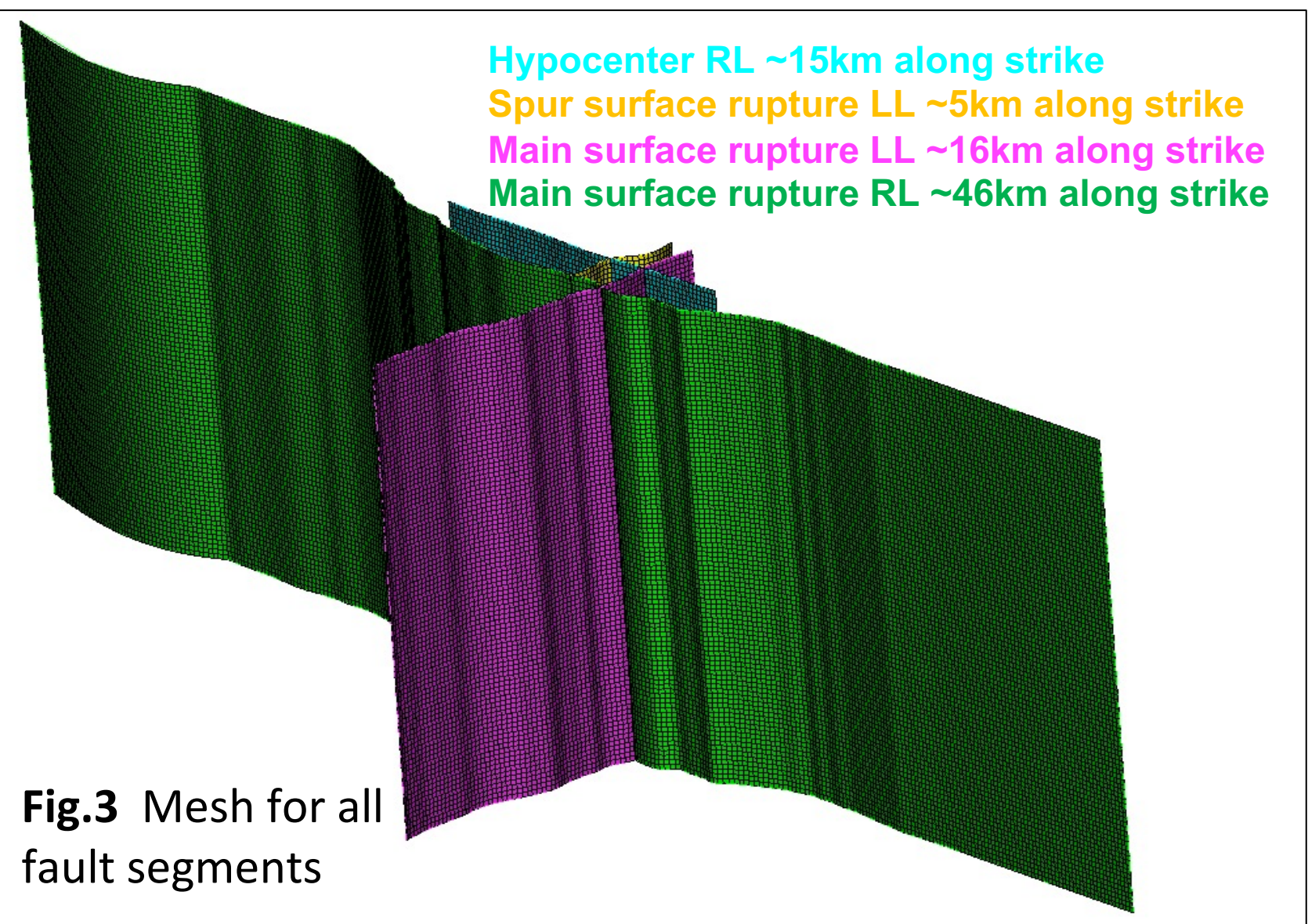


Fig. 3 Mesh for all fault segments

PARAMETER	VALUE
STATIC COEFF FRICTION	0.6
DYNAMIC COEFF FRICTION	0.1
SHEAR STRESS ALONG STRIKE	2.3 MPa
SHEAR STRESS ALONG DIP	0 MPa
NORMAL STRESS	6 MPa
SLIP WEAKENING DISTANCE	0.12 m

Table 1. Initial conditions for the homogeneous M7.1 earthquake model.

M6.4 homogeneous model

Produces heterogeneous pre-stress for M7.1 model

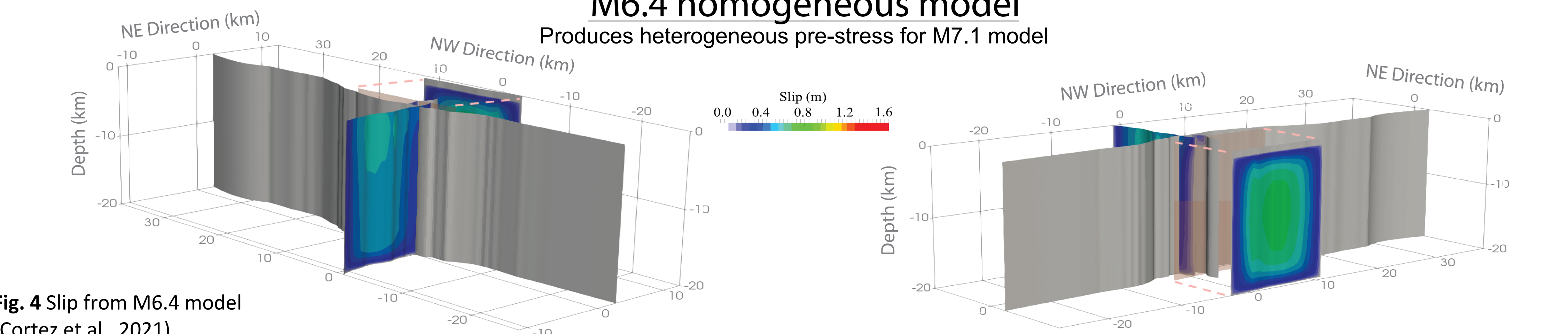


Fig. 4 Slip from M6.4 model (Cortez et al., 2021)

M7.1 input stresses

homogeneous stress

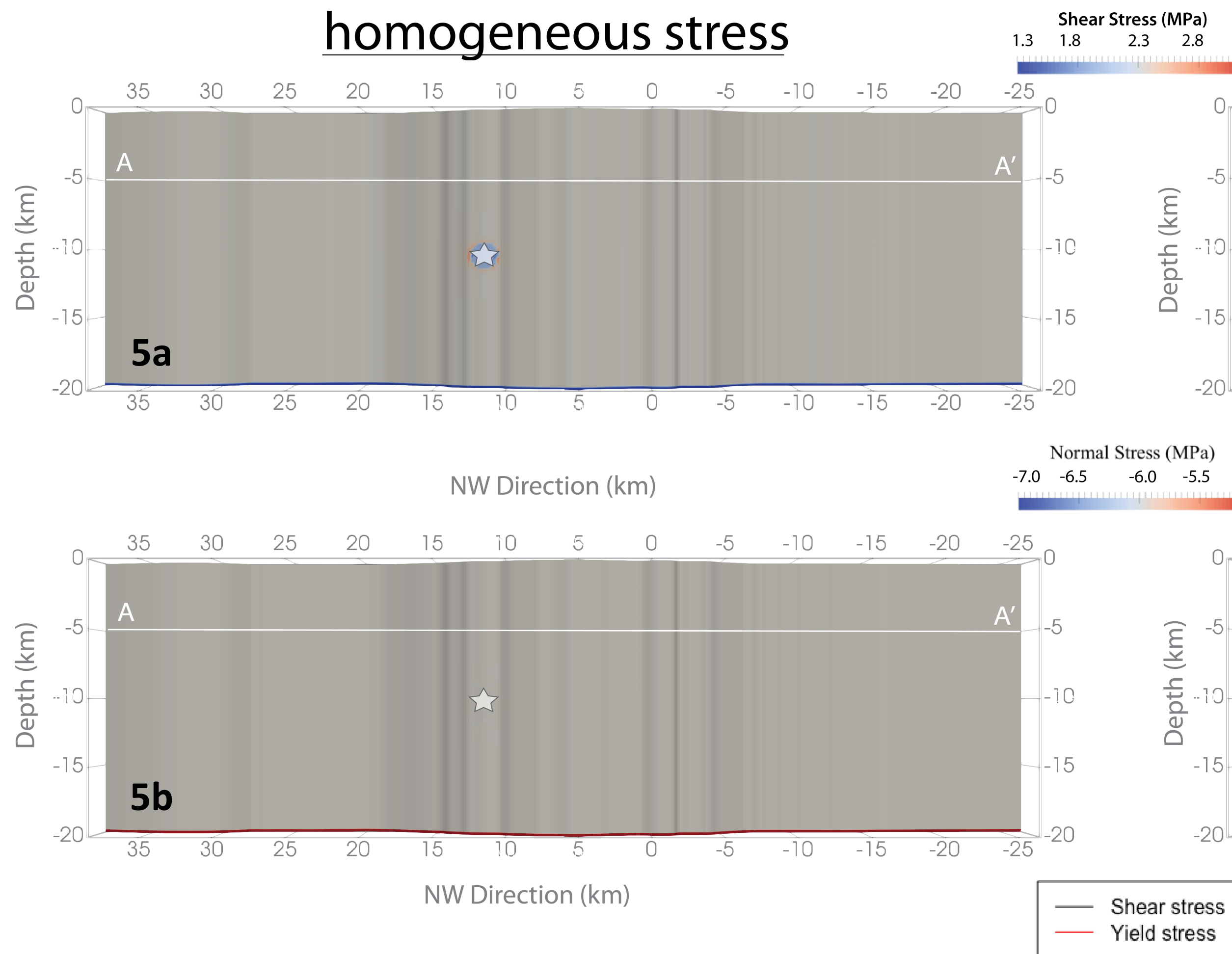


Fig. 5a Initial shear and normal stresses for the M7.1 homogeneous model.

M6.4 residual stress

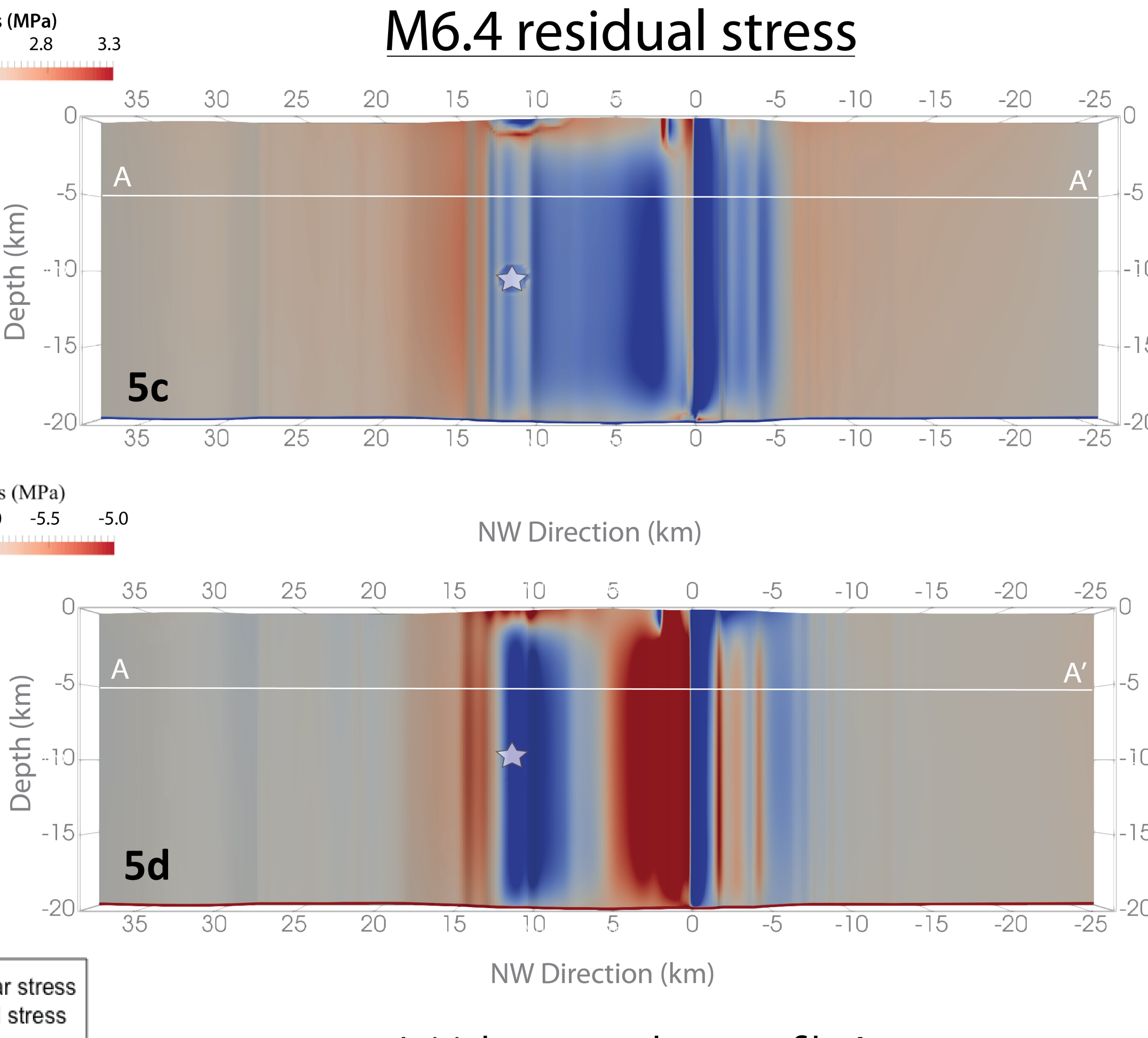


Fig. 5c Initial shear and normal stresses for the M7.1 heterogeneous model using residual stress from the M6.4 event.

Initial stresses along profile A

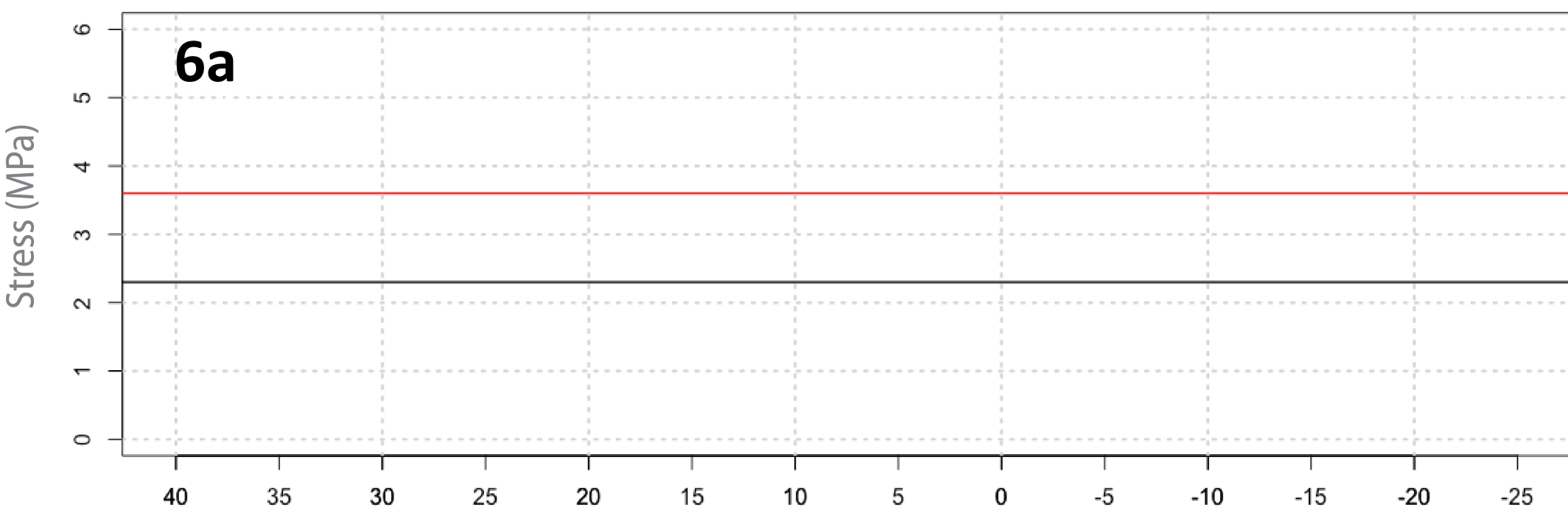


Fig. 6a Final slip patterns for both models.

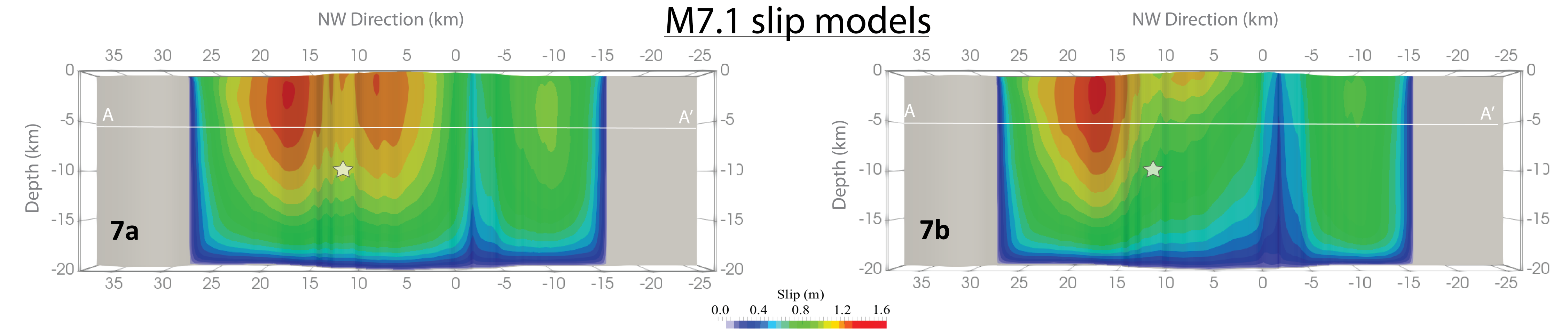
Initial stresses along profile A



Fig. 6b Final slip patterns for both models.

Results

M7.1 slip models



Figs. 4a & 4b Initial shear and normal stresses for the M7.1 homogeneous model. **Figs. 4c & 4d** Initial shear and normal stresses for the M7.1 heterogeneous model using residual stress from the M6.4 event. Note stress shadowing due to slip on the right-lateral segment of the M6.4 event. **Figs. 5a & 5b** Initial shear and yield ($\mu_{static}\sigma_n$) stress for M7.1 models along profile A. **Figs. 6a & 6b** Final slip patterns for both models. Note effects of stress shadowing in the heterogeneous model (6b), with less slip in the areas shadowed by the M6.4 event.

Discussion of results

Slip on the earlier M6.4 fault (fig 4) caused shear stress shadowing in certain areas of the M7.1 fault as shown in fig. 5c.

Both homogenous (figs 5a & 5b) and heterogeneous (figs 5c & 5d) models of the M7.1 result in heterogeneous slip patterns that qualitatively match geodetic and seismic inversions, with slightly better match from the heterogeneous model.

Conclusions

Our models show that both fault geometry and transferred stress from the prior event likely had strong effects on the slip distribution of the M7.1 Ridgecrest earthquake. In the future, incorporating rate and state friction and realistic fault geometry will better illustrate the time-dependent stress transfer within the fault system.

References

- Barall, M. (2009), A grid-doubling technique for calculating dynamic three-dimensional spontaneous rupture on an earthquake fault, *Geophysical Journal International*, 178, 845-859.
- Cortez, J. T., D. D. Oglesby, C. Kyriakopoulos, B. Wu, K. Chaudhuri, A. Ghosh, and R. Douilly (2021), On the rupture propagation of the 2019 M6. 4 Searles Valley, California, Earthquake, and the lack of immediate triggering of the M7. 1 Ridgecrest Earthquake, *Geophysical Research Letters*, 48(4), e2020GL090659
- Ji, C., D.J. Wald, and D.V. Helmberger (2002), Source description of the 1999 Hector Mine, California earthquake; Part I: Wavelet domain inversion theory and resolution analysis, *Bull. Seism. Soc. Am.*, Vol 92, No. 4, pp. 1192-1207
- Li, C., G. Zhang, X. Shan, D. Zhao, Y. Li, Z. Huang, R. Jia, J. Li, and J. Nie (2020), Surface Rupture Kinematics and Coseismic Slip Distribution during the 2019 Mw7.1 Ridgecrest, California Earthquake Sequence Revealed by SAR and Optical Images, *Remote Sensing*, 2020; 12(23):3883.



Acknowledgements

Keith Richards-Dinger
Katherine Kendrick
Feng Hu